

Ultrahigh-Resolution Electron Microscopy of Charge-Density Waves in $2H$ -TaSe₂ below 100 K

J. M. Gibson, C. H. Chen, and M. L. McDonald

Bell Laboratories, Murray Hill, New Jersey 07974

(Received 22 July 1982; revised manuscript received 22 March 1983)

Ultrahigh-resolution transmission-electron micrographs display $3a_0$ periodic distortions of the crystal lattice in $2H$ -TaSe₂ associated with charge-density waves below 120 K. Approximate structure-factor magnitudes and signs within single domains of the commensurate phase are determined. The data fit well only one of the models recently derived from ⁷⁷Se NMR. The charge-density-wave amplitude is 30% less in the orthorhombic direction for this model. The center of symmetry within the orthorhombic unit cell is determined. Images from incommensurate phases are discussed.

PACS numbers: 61.16.Di, 61.55.Hg

Recent dark-field electron-microscopical evidence¹⁻³ on the real-space nature of charge-density wave (CDW) atomic displacements in $2H$ -TaSe₂ has had considerable impact on the subject. While initially confirming the discommensurate nature of the incommensurate states between 90 and 120 K,¹ proposed by McMillan⁴ and elegantly deduced from diffraction data by Fleming *et al.*,⁵ more detailed work revealed significant differences from the expected microstructures, especially during cooling.^{2,3} Undoubtedly the most significant and surprising finding, made with use of convergent-beam electron diffraction within one domain of the commensurate state,² was that the local symmetry of the CDW states appears to be orthorhombic and not hexagonal. Using NMR of ⁷⁷Se nuclei, Pfeiffer *et al.*⁶ have since confirmed this finding and produced several qualitatively different models of the CDW amplitudes and phases which fit their data. Theoretical discussions of the orthorhombic distortion have been given by Walker and Jacobs,⁷ Littlewood and Rice,⁸ and McMillan.⁹

In this Letter we present data obtained from ultrahigh-resolution electron microscopy of $2H$ -TaSe₂ below 100 K. A liquid-He-cooled specimen stage with exceptionally high mechanical stability was constructed for a JEOL 200-kV ultrahigh-resolution electron microscope to make these experiments possible.¹⁰ This instrument has a point-to-point resolution of 2.5 Å, allowing faithful imaging in thin specimens of the $\langle 10\bar{1}0 \rangle$ lattice period (2.97 Å) and the $\frac{1}{3}\langle 10\bar{1}0 \rangle$ (8.91 Å) and $\frac{2}{3}\langle 10\bar{1}0 \rangle$ (4.46 Å) CDW displacement periods. Only those diffracted beams with $|g| (= 1/d) < 0.4 \text{ \AA}^{-1}$ were permitted by the objective aperture to contribute to the image.

In high-resolution electron microscopy, unlike diffraction or dark-field techniques, the relative

phase of diffracted beams can be directly revealed. Apart from making possible the detailed study of regions of rapidly varying phase (such as discommensurations) this allows us under restricted conditions to identify the phase of Fourier components of the lattice potential for crystal-structure determination. In the presence of multiple-scattering the phase of diffracted beams is only simply related to that of Fourier coefficients if the crystal possesses a center-of-symmetry. Fung *et al.*² demonstrated that the space group $Cmcm$, which is centrosymmetric, appears to best describe orthorhombic $2H$ -TaSe₂. This is furthermore one of only six possible groups consistent with Landau theory.⁹ From Freidel's law centrosymmetric lattices have real Fourier coefficients. For the case of $2H$ -TaSe₂, then, the problem of determining the phase of the Fourier coefficients is simply a sign determination. Provided the thin samples are sufficiently well oriented axially, the effects of electron multiple scattering and microscope transfer function on image amplitudes are factors of $\exp(in\pi)$ (n integral), which can generally be easily determined experimentally.¹¹

Thin samples were prepared for high-resolution electron microscopy (HREM) by repeated cleaving normal to the c axis with soluble adhesive tape and were supported on fine-mesh copper grids. Regions in the vicinity of the sample edge were acceptably thin and could be found in the zone-axis orientation as a result of local sample buckling. A heater and thermocouple on the specimen holder were used to control and measure temperature. Optical diffraction patterns taken from disordered areas on HREM negatives were used to determine the microscope operating conditions and select images taken sufficiently close to the Scherzer focus.¹¹ Image calculations

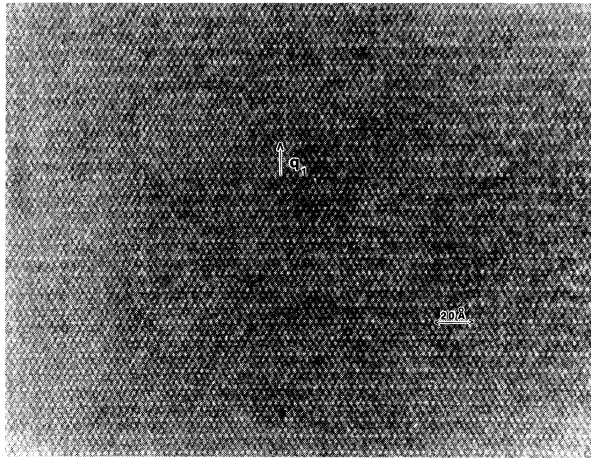


FIG. 1. An HREM picture of $2H$ -TaSe₂ in its commensurate CDW state at 60 K showing a strong $3a_0$ modulation in the CDW q_1 direction. This image is typical of thick ($> 200 \text{ \AA}$) specimen areas.

were made with a multislice approach¹² to take full account of multiple scattering and microscope transfer function. Local thickness could be determined by direct comparison of calculated and real images, noting the location of "fringe reversals." This procedure was often frustrated by the rather abrupt thickness changes characteristic of cleaved layer compounds.

Figure 1 is an HREM picture, taken at 60 K, well within one commensurate domain of $2H$ -TaSe₂. It was chosen because it most clearly demonstrates a CDW modulation (q_1), of period $3a_0$, to the unaided eye. In these experiments a primary difficulty is that the CDW modulations are rather weak and show up most dramatically in thicker specimen areas ($> 200 \text{ \AA}$), where multiple scattering and possible slight specimen misorientation are most critical. The one-dimensional appearance of Fig. 1, which is typical of thick areas, is therefore misleading. Figure 2, taken at 40 K, is characteristic of regions whose thickness is less than 130 \AA but greater than 35 \AA . In such images, taken near the Scherzer focus, it can be shown by numerical simulation that white dots correspond to Ta atom strings in the object. In Fig. 2 the CDW modulations are not so readily visible to the eye because of the presence of noise, mostly arising from surface contamination. Nevertheless, calculations show that in this thickness regime the weak CDW diffraction is "kinematical" and so closely related to the CDW structure factors, which we wish to obtain. Analysis is aided in thin specimen areas by optical

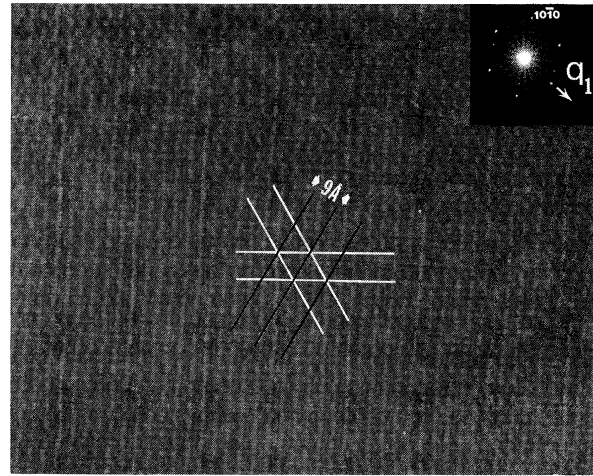


FIG. 2. An HREM picture of $2H$ -TaSe₂ at 40 K where specimen thickness is less than 130 \AA . The CDW modulations are weak and cannot be readily seen by eye. The dark and light ruled lines indicate the position of minima and maxima (respectively) in these modulations determined from optical densitometry of the negative (e.g., Fig. 3). Inset: An optical diffraction pattern from a somewhat thicker specimen area displaying the relative amplitudes of the CDW modulation in the image (effective area sampled is 1000 \AA^2). The optical diffraction method also confirms that the image was exposed near the Scherzer focus condition.

densitometry using a slit scanned in the CDW q direction, which averages over noise perpendicular to q . A trace from Fig. 1 is shown in Fig. 3, clearly revealing the strong $3a_0$ q_1 modulation.

By simple Fourier analysis of such traces the amplitudes and phases of the CDW image components in thin regions have been identified. Since

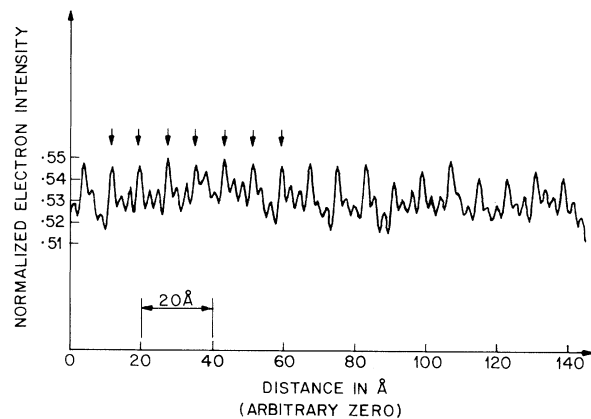


FIG. 3. An optically obtained trace of the electron intensity on the negative of Fig. 1 scanned in the q_1 direction with a slit of effective dimensions 30 and 1 \AA^2 .

these images were taken under axial conditions near the Scherzer focus (demonstrated by optical-diffraction patterns like the inset in Fig. 2) and the crystal is centrosymmetric, the sign (or phase) of the image components is the same as that of the projected-potential Fourier components, or structure factors, for thickness $35 < t < 130$ Å. Image calculations have also confirmed that the CDW diffracted amplitudes are also proportional to the structure factors for $t < 130$ Å (this is an advantage of the weakness of the modulations). Our experimental observations from suitably thin areas show that two $\frac{1}{3}\langle 10\bar{1}0 \rangle$ Fourier components have the same sign as the lattice $\langle 10\bar{1}0 \rangle$ potential fluctuation (which is a maximum at Ta strings) and the third (orthorhombic direction) has opposite sign. This information is summarized graphically in Fig. 2. The existence of local orthorhombic symmetry is confirmed by the observed signs of CDW Fourier components.

In order to facilitate the analysis of this data in terms of the real CDW's we have calculated structure factors for the NMR-derived CDW parameters of Pfeiffer *et al.*⁶ Each of their six models (below 80 K) provides two CDW amplitudes ρ_1 and ρ_2 and phases φ_1 and φ_2 for the orthorhombic direction and the other two directions, respectively. We differentiate the CDW's to determine atomic displacements within one layer. Since there are three inequivalent centers of symmetry possible for the combination of two layers, there are eighteen possible real-space models, whose Fourier components are tabulated in Table I. The three centers of symmetry (COS in Table I) lie along the orthorhombic distortion direction: (1) at the unit cell origin between Ta's in adjacent layers; (2) $0.866a_0$ from the origin (above a Se site); and (3) $1.732a_0$ from the origin (another Ta site). All three are centers for the $2H$ -TaSe₂ subcell and are the only inequivalent positions allowed by symmetry. Note that the structure factors do not display a simple relationship to the CDW amplitudes in different directions. This is a consequence of the large number of atoms within the CDW unit cell (54).

Our experimental data both from analysis of optical-density traces and optical diffraction patterns (such as the inset in Fig. 2) from single domains in thin specimen areas reveals that all three $\frac{1}{3}\langle 10\bar{1}0 \rangle$ Fourier components have equal amplitudes within 20%. Their absolute magnitudes are less accurately known, since they depend on thickness and the instrument transfer function. They are estimated to be between 0.2 and 0.4 of

TABLE I. Calculated structure factors (at 50 K) for the NMR-derived CDW models of Pfeiffer *et al.* (Ref. 6). F_1 and F_2 are the ratios of the $\frac{1}{3}\langle 10\bar{1}0 \rangle$ and $\langle 10\bar{1}0 \rangle$ structure factor amplitudes in the orthorhombic and the other two directions, respectively. G_1 and G_2 are similar ratios for $\frac{2}{3}\langle 10\bar{1}0 \rangle$. These scale with the absolute amplitudes of the displacements and were calculated for a displacement wave of amplitude in Å equal to the CDW amplitudes ρ_1 and ρ_2 as published (Ref. 6) (e.g., for solution 4 at 50 K this is 0.023 Å). Missing entries in the table are smaller than 0.5×10^{-2} .

Model	ρ_1/ρ_2	COS	10^2F_1	10^2F_2	10^2G_1	10^2G_2
1	6.7	1	7.8	-0.7	-7.3	-0.5
		2	-9.3	•••	-2.9	-0.1
		3	1.5	1.1	10.3	-0.5
2	6.7	1	9.1	-1.1	-8.2	•••
		2	-9.2	0.7	-3.4	-0.5
		3	•••	•••	11.6	-0.9
3	0.69	1	-2.8	-5.1	-0.9	-1.5
		2	-0.8	-0.5	3.5	-6.4
		3	3.5	5.6	-2.6	-4.9
4	1.0	1	-2.0	-3.8	-1.9	-1.6
		2	-2.6	-1.1	3.9	-5.3
		3	4.6	4.9	-2.1	-3.7
5	1.0	1	•••	2.3	-2.3	2.7
		2	-3.6	2.2	2.5	3.0
		3	3.8	-4.4	•••	•••
6	0.69	1	1.5	1.8	-2.2	4.3
		2	-3.3	3.6	0.5	3.8
		3	1.8	-5.4	1.7	-0.6

the $\langle 10\bar{1}0 \rangle$ structure factor. The $\frac{2}{3}\langle 10\bar{1}0 \rangle$ components have comparable magnitudes excepting that the orthorhombic direction has a somewhat smaller amplitude than the others. However, this last measurement is particularly difficult to quantify because of multiple interference effects in HREM images.¹¹

Examining Table I, we can rapidly rule out the "one-dimensional" CDW models 1 and 2 (but note that the Fourier components do not always display comparable asymmetry, e.g., model 1, COS 3). On the sole basis of the $\frac{1}{3}\langle 10\bar{1}0 \rangle$ structure factor measurements we would choose model 4, COS 3, model 5, COS 3, or model 6, COS 1 or 2. However, only model 6 with center of symmetry 2 fits both the experimentally determined signs of the $\frac{1}{3}\langle 10\bar{1}0 \rangle$ components and the sense of the $\frac{2}{3}\langle 10\bar{1}0 \rangle$ amplitudes. This model also intuitively fits the sense of contrast seen in thick areas, where dark-field images show domains as dark in their orthorhombic direction diffraction spots.^{2,3} (Dynamical calculations show that this effect is preserved in thick regions but is sensitive to ex-

act orientation as reported.³) In this model the CDW amplitudes are $\rho_1 = 0.69\rho_2$ and phases $\varphi_1 = 1.4$ and $\varphi_2 = 5.2$ rad (relative to a Ta atom in one layer) at 50 K. It should be noted that the detailed structure factors are sensitive also to the "square amplitude" estimated by Pfeiffer *et al.*⁶

Images taken in the incommensurate states do not easily reveal structure at discommensurations because of the weakness of CDW modulations in thin areas and the complexities of multiple scattering in thicker areas. However, it appears that CDW amplitudes fall off within one or two periods (20 Å) of discommensurations and we see no obvious evidence for a hexagonal phase at discommensuration cores.⁸ We cannot rule out the alternative possibility that discommensurations have a small vibrational amplitude of this order. Between discommensuration cores the CDW structure appears qualitatively similar to that discussed above.

In conclusion, we have demonstrated local orthorhombic symmetry in a single unit cell of the commensurate state of *2H-TaSe₂* below 80 K. We have deduced that a model in which the CDW in the orthorhombic direction has 0.69 of the amplitude of the other two is most likely in this temperature regime. We estimate the amplitude of the displacement waves at 0.2 Å. We note that this is a significant deviation from a hexagonal

model. The center of symmetry between layers appears to lie above a Se atom position.

We gratefully acknowledge the assistance of R. M. Fleming, T. Kovacs, and D. Garcia and productive discussions with L. N. Pfeiffer and P. B. Littlewood.

¹C. H. Chen, J. M. Gibson, and R. M. Fleming, *Phys. Rev. Lett.* **47**, 723 (1981).

²K. K. Fung, S. McKernan, J. W. Steeds, and J. A. Wilson, *J. Phys. C* **14**, 5417 (1981).

³C. H. Chen, J. M. Gibson, and R. M. Fleming, *Phys. Rev. B* **26**, 184 (1982).

⁴W. L. McMillan, *Phys. Rev. B* **14**, 1496 (1976).

⁵R. M. Fleming, D. E. Moncton, D. B. McWhan, and F. J. DiSalvo, *Phys. Rev. Lett.* **45**, 576 (1980).

⁶L. N. Pfeiffer, R. E. Walstedt, R. F. Bell, and T. Kovacs, *Phys. Rev. Lett.* **49**, 1162 (1982).

⁷M. E. Walker and A. E. Jacobs, *Phys. Rev. B* **24**, 6770 (1982).

⁸P. B. Littlewood and T. M. Rice, *Phys. Rev. Lett.* **48**, 27 (1982).

⁹W. L. McMillan, to be published.

¹⁰J. M. Gibson and M. L. McDonald, to be published.

¹¹See, for example, J. C. H. Spence, *Experimental High-Resolution Electron Microscopy* (Oxford Univ. Press, New York, 1980).

¹²J. M. Cowley and A. F. Moodie, *Acta Crystallogr.* **10**, 609 (1957).

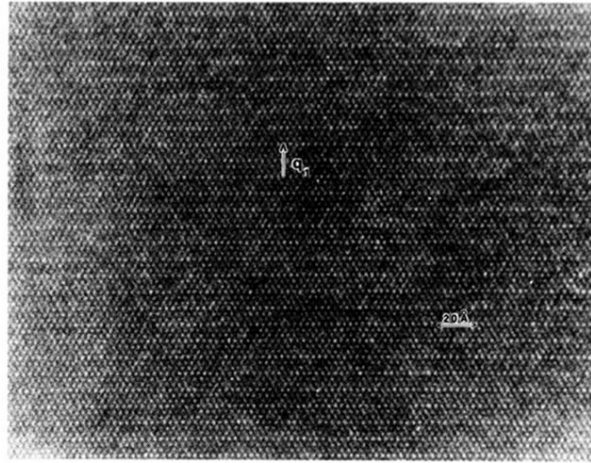


FIG. 1. An HREM picture of $2H\text{-TaSe}_2$ in its commensurate CDW state at 60 K showing a strong $3a_0$ modulation in the CDW q_1 direction. This image is typical of thick ($> 200 \text{ \AA}$) specimen areas.

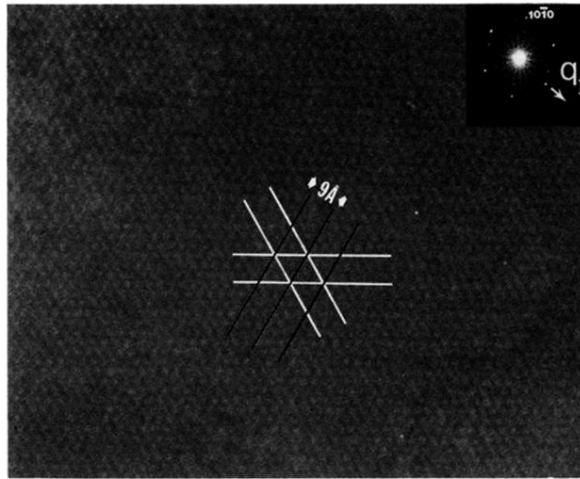


FIG. 2. An HREM picture of $2H$ -TaSe₂ at 40 K where specimen thickness is less than 130 Å. The CDW modulations are weak and cannot be readily seen by eye. The dark and light ruled lines indicate the position of minima and maxima (respectively) in these modulations determined from optical densitometry of the negative (e.g., Fig. 3). Inset: An optical diffraction pattern from a somewhat thicker specimen area displaying the relative amplitudes of the CDW modulation in the image (effective area sampled is 1000 Å²). The optical diffraction method also confirms that the image was exposed near the Scherzer focus condition.